Electric fields and electron energies in sprites and temporal evolutions of lightning charge moment

T Adachi[1], Y Hiraki[2], K Yamamoto[3], Y Takahashi[3], H Fukunishi[3], R-R Hsu[4], H-T Su[4], A B Chen[4], S B Mende[5], H U Frey[5] and L C Lee[6]

[1] Research Institute for Sustainable Humanosphere, Kyoto University, Uji, Kyoto, Japan
[2] Solar-Terrestrial Environment Laboratory, Nagoya University, Nagoya, Aichi, Japan
[3] Department of Geophysics, Tohoku University, Sendai, Miyagi, Japan
[4] Department of Physics, National Chen Kung University, Tainan, Taiwan
[5] Space Sciences Laboratory, University of California at Berkeley, USA
[6] Institute of Space Science, National Central University, Chungli, Taiwan

E-mail: tadachi@rish.kyoto-u.ac.jp

Abstract

The fundamental electrodynamical coupling processes between lightning and sprites are investigated. By combining the observed spectral data with the Monte Carlo swarm experiments, reduced electric fields and electron energies in sprite streamers and halos are estimated. The obtained fields inside sprite halos (70–97 Td with an analysis error of ± 5 Td) are lower than the conventional breakdown field, $E_k \sim 128$ Td, indicating a significant reduction of electrons associated with halos while those in sprite streamers (98–380 Td with an error of ± 50 Td) are higher than E_k, suggesting that a significant ionization process drives their formation and development. A combined analysis of photometric and electromagnetic data makes it possible to estimate temporal evolutions of lightning charge moment. It is found that lightning discharges with a short time scale (~ 1 ms) and a moderate amount of charge moment (~ 400 C km) produce discernible halos. On the other hand, lightning discharges with a large amount of charge moment (~ 1300 C km) produce streamers regardless of their time scale. The results obtained are comprehensively interpreted with both the conventional breakdown field necessary for the formation of streamers and the electric field necessary for the production of optical emissions of halo which is sensitive to the time scale of the thundercloud field due to the significant reduction of electrons.

1. Introduction

Sprites and halos are transient optical phenomena at mesospheric altitudes produced by lightning discharges. Past imaging observations have clarified their morphological properties in details. Sprites are usually composed of a cluster of vertical columns, sometimes accompanied by downward and upward branching structures which form a carrot-like shape at 50–90 km altitudes. (e.g. Sentman *et al* 1995, Cummer *et al* 2006a). Telescopic observations have clarified that sprites consist of fine structures with typical diameters ranging from a few tens to a few hundreds of metres (e.g. Gerken *et al* 2000, Gerken and Inan 2002),

which are considered to be streamer type air discharges (e.g. Pasko *et al* 1998, Liu and Pasko 2004). It has also been found that a clear morphological transition exists between the upper-diffuse region and the lower-structured region (e.g. Pasko and Stenbaek-Nielsen 2002). At the altitudes of the diffuse region, a pancake-like diffuse glow referred to as a sprite halo is often observed. Sprite halo occurs at altitudes of 75–85 km with horizontal extents of 60–90 km (e.g. Barrington-Leigh *et al* 2001, Wescott *et al* 2001, Miyasato *et al* 2002). Although past imaging observations have indicated that sprites and halos are independent phenomena (e.g. Moudry *et al* 2003), electrodynamical coupling processes between lightning and each phenomenon are not yet fully understood.

Therefore, comprehensive experiments such as coincident imaging, spectral and electromagnetic measurements are required.

Spectral measurements of sprites have identified the first positive band ($B\,^3\Pi_g \rightarrow A\,^3\Sigma_u^+$) and second positive band ($C\,^3\Pi_u \rightarrow B\,^3\Pi_g$) of nitrogen molecules as the primary emission source of observed red and blue light, respectively (Mende *et al* 1995, Hampton *et al* 1996, Suszcynsky *et al* 1998). Further measurements have found the possible presence of the Meinel band ($A\,^2\Pi_u \rightarrow X\,^2\Sigma_g^+$) and first negative band ($B\,^2\Sigma_u^+ \rightarrow X\,^2\Sigma_g^+$) of nitrogen ions (Morrill *et al* 1998, Suszcynsky *et al* 1998). Spectral analysis using kinetic models has been used for the estimation of electron energies and reduced electric fields producing optical emissions of sprites. Studies based on ground-based spectral measurements have demonstrated that Boltzmann electron temperatures are in the range 0.4–10 eV (Green *et al* 1996, Miyasato *et al* 2003), although the atmospheric attenuation effect causes inevitable uncertainty in these analyses. For a more accurate estimation, spectral measurements have been carried out from higher altitudes where atmospheric attenuation is negligible. It has been reported that the spectral information obtained by the ISUAL payload on the FORMOSAT-2 satellite are consistent with those produced under reduced electric fields of 2.1–3.7 E_k (average electron energy of 6.2–9.2 eV) where E_k of $\sim$128 Td (1 Td = 10^{-17} V cm^2) is the conventional breakdown field, which probably reflect the electric fields in the head of individual streamers (Kuo *et al* 2005, Liu *et al* 2006).

On the other hand, electromagnetic observations have been carried out to clarify the electrical properties of sprite-producing lightning discharges. It has been demonstrated that electromagnetic waves in the range of very low frequency (VLF: 3–30 kHz) and extremely low frequency (ELF: 3 Hz–3 kHz) contain larger low-frequency energy than those of ordinary lightning, which is suggestive of long-lasting currents and a large amount of charge moment change (the product of charge and its height) in lightning. Experimental studies based on Schumann resonance (SR) (e.g. Sentman 1966) data have estimated time-integrated charge moment changes of 200–2000 C km in sprite-producing lightning (e.g. Huang *et al* 1999, Füllekrug and Reising 1998, Hobara *et al* 2001, Sato and Fukunishi 2003). In contrast to the SR data, ELF/VLF atmospherics data are useful to derive the temporal evolution of charge moment changes. It has been demonstrated that charge moment changes before the initiation of sprites are from 250 to 3250 C km (e.g. Cummer and Inan 1997). Recent statistical study has clarified that the threshold of sprite generation is in the range 600–1000 C km (Hu *et al* 2002). However, the results obtained are in a wide range and further experiments are required to study how the diversity of lightning charge moment affects the electrodynamical processes in sprites.

The purpose of this study is to estimate macroscopic parameters such as the electron energies and electric fields in sprites and the charge moment changes of their parent lightning discharges and to comprehensively understand their fundamental coupling processes.

## 2. Instrumentation and observation

2.1. FORMOSAT-2/ISUAL

The FORMOSAT-2 satellite (previously known as ROCSAT-2) is a Taiwanese satellite carrying two payloads: the Remote Sensing Instrument (RSI) and the Imager for Sprites and Upper Atmospheric Lightning (ISUAL) (Chern *et al* 2003, Frey *et al* 2005, 2007, Kuo *et al* 2005, Mende *et al* 2005, Adachi *et al* 2006). It flies on a sun-synchronous (9:30 and 21:30 local time) polar-orbit at an altitude of $\sim$891 km with a period of 14 revolutions per day. The ISUAL consists of an imager with a selectable six-colour filter wheel, a six-colour spectrophotometer (SP) and a dual-colour array photometer (AP). It looks at the Earth's limb direction and observes upper atmospheric optical phenomena such as sprites, elves and gigantic jets under nighttime conditions. In order to maximize the detection probability using the limited data storage, the ISUAL data recording is performed when the output signal level of SP exceeds a certain pre-programmed trigger criterion.

In this study, optical data obtained with the imager and AP is primarily analysed. The imager has a field-of-view (FOV) of 20° (horizontal) × 5° (vertical) corresponding to an area of 1084 km × 271 km at the limb point 3106 km away from the satellite. The spatial resolution corresponds to $\sim$2 km at the limb while temporal resolution is programmable in the range 1–1000 ms. In this analysis, all the sprite images are taken through the 633–751 nm band pass filter with an exposure time of 30 ms. On the other hand, the AP consists of two multi-channel photometers measuring two different wavelength ranges 340–480 and 510–750 nm selected by blue and red broadband filters, respectively (see figure 5). The sensor is a multi-anode photomultiplier that has sixteen aligned anodes. The FOV of each channel is 22° (horizontal) × 0.23° (vertical) and the whole FOV is 22° (horizontal) × 3.6° (vertical). Thus, the AP has a vertical resolution of $\sim$14 km at the limb point, which enables us to separately detect optical emissions of sprites and lightning. The AP data are recorded at a sampling frequency of 20 kHz for the initial 10/18 ms and are recorded at a frequency of 2 kHz for the following 230/222 ms.

2.2. ELF magnetometer

For the estimation of lightning charge moment changes, lightning-induced transient SR data measured at the Onagawa observatory (38.4°S, 141.5°E) are analysed. At this observatory, two orthogonal search coil magnetometers with two pre-amplifiers are installed for the measurements of geomagnetic north–south and east–west magnetic field components. The output signals are led to a main amplifier that has a gain of $\sim$46 dB. In order to reject artificial power line noises, three notch filters are used. These filters attenuate signals at frequencies of 50, 100 and 150 Hz to $-$60 dB with Q-factors of $\sim$2. The output signals of the main amplifiers are then converted to 16-bit digital data with a sampling rate of 400 Hz by an analog-to-digital converter board and continuously recorded on a personal computer. Consequently, the system provides a flat sensitivity of 60 mV pT^{-1} in a
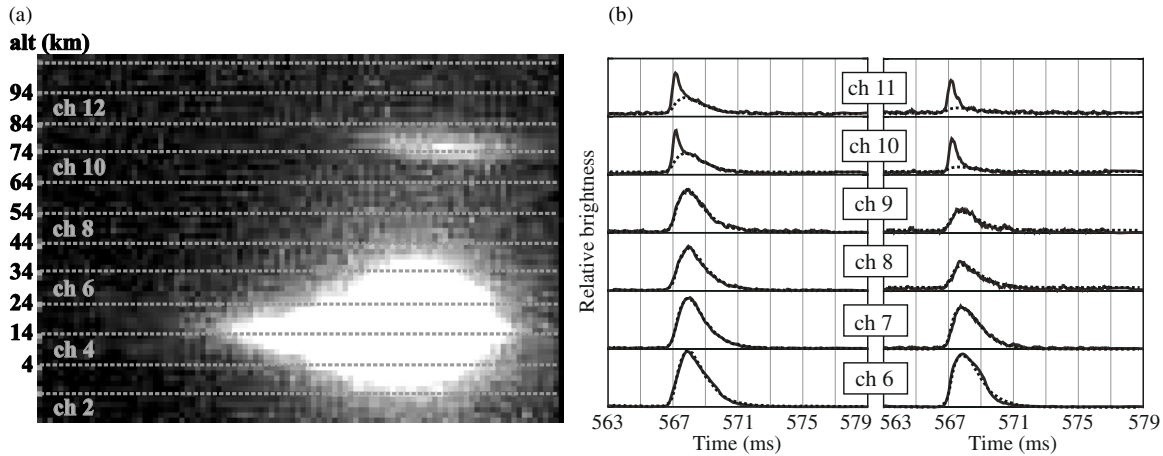
Figure 1. (*a*) An image of halo event observed with the ISUAL imager at 04:40:25.552-581 (UT) on 9 October 2005. Grey dotted lines demonstrate the fields of view of the AP. (*b*) Concurrent AP data in the blue (left) and red (right) channels. Solid lines show original output signals while dotted lines represent lightning contamination at each channel.

frequency range 7–90 Hz, which enable us to detect both the continuous SR excited by global lightning activity and the transient SR waves related to extremely large lightning events. Because signals from magnetometers are recorded with a GPS time code, it is possible to investigate the one-to-one relationship between the sprite events observed with ISUAL and the transient SR events monitored at the Onagawa observatory.

2.3. Classification of sprite events

During the period from 4 July, 2004 to 25 June 2006, the ISUAL observed 482 sprite events. These events are classified into three categories: halo events, halo-streamer events and streamer events. Based on past imaging studies (e.g. Sentman *et al* 1995, Wescott *et al* 1998, 2001), a pancake-like diffuse emission with a lateral extent of >50 km is identified as a sprite halo while the vertically oriented structures with a length of >10 km are identified as sprite streamers. Because the spatial resolution of the ISUAL imager is ∼2 km, streamer structures of 10 km lengths correspond to ∼5 pixel elements on the CCD image, which are distinguishable from background noises. Consequently, we obtain 128 halo events, 126 halo-streamer events, 206 streamer events and 22 unclassified events.

Figure 1(*a*) shows imager data of a halo event observed at 04:40:25 (UT) on 9 October 2005. Horizontal dotted lines represent the FOV of individual AP channels. A halo is seen in channels 10 and 11 while a bright emission of the parent lightning flash is seen in channels 3–7. Figure 1(*b*) represents concurrent AP data (solid lines), in which background emissions are subtracted. By scaling the lightning signal in channel 1 (not shown) to the signals in channels 6–11, lightning contamination is estimated at each channel (dotted lines). Since channels 6–9 point below the altitude of halo, temporal variations in these photometer channels are primarily due to scattering light from the parent lightning flash. On the other hand, sharp impulsive signals are found in channels 10 and 11 at 04:40:25.567 (UT). Because such signatures cannot be seen in channels 6–9, these peaks are probably due to the halo

emissions. Consequently, it is found that the optical emission of halo starts with a delay time of ∼0.1 ms and lasts for ∼1 ms. Here, the delay time is defined as the time difference between the initiations of lightning and halo, and the initiation time is defined when the signal for the first time exceeds a level 10 times higher than the standard deviation (σ) of background noise.

Figure 2(*a*) shows imager data of a halo-streamer event observed at 14:53:13 (UT) on 3 October 2005. The figure format is the same as that of figure 1. A horizontally elongated bright emission seen in channels 8–10 is a lightning flash. On the other hand, a pancake-like emission of a sprite halo accompanied by several streamer structures extended downwards from its bottom is seen in channels 12–14. Figure 2(*b*) represents concurrent AP data. All signals observed through the blue filter reach saturation levels, which are due to extremely bright emissions of the parent lightning flash. Since most of the halo-streamer events have similar characteristics, it is suggested that lightning discharges in this category are much more energetic than those in the other categories. However, sprite signals are seen in the red photometer channels, which have durations ranging from 0.7 to 1.5 ms. From time differences between peaks in each channel, the downward propagation speed of sprite streamers is estimated to be ∼7×10^7 m s^{-1}.

Figure 3(*a*) represents an imager data of a streamer event observed at 21:31:27 (UT) on 14 October 2004. The figure format is the same as that of figures 1 and 2. A bright optical emission seen in channel 1 and below it is a lightning flash while two vertically oriented structures in channels 2–6 are sprite streamers. Figure 3(*b*) shows concurrent AP data with solid lines and estimated lightning contamination with dotted lines. The emission peaks seen at 945–948 ms probably correspond to the optical emissions of sprite streamers. In this event, streamers start in channel 5 with a delay time from the parent lightning of ∼2 ms and subsequently propagate upwards to channel 6 and downwards to channels 3–4 with a velocity of 2×10^7–1.1×10^8 m s^{-1}.
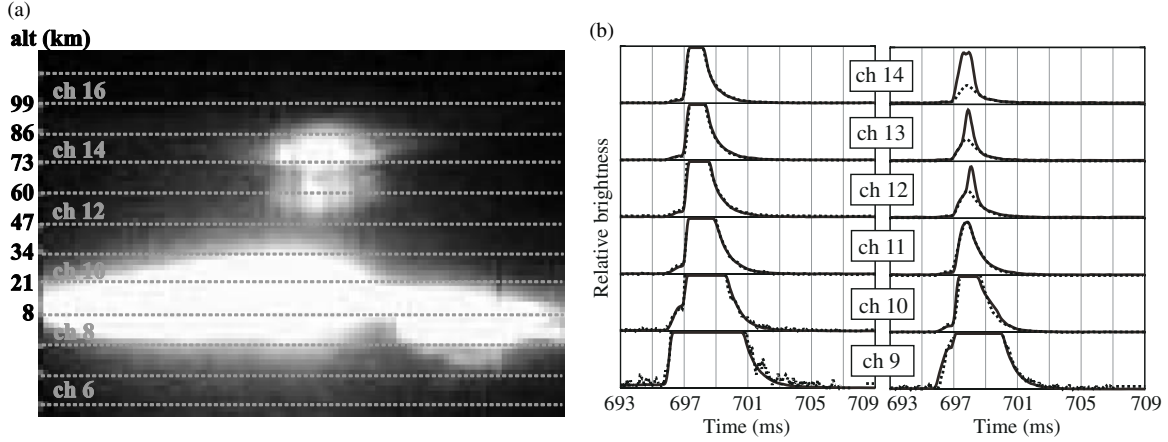
Figure 2. (*a*) An image of halo-streamer event observed at 14:53:13.687-716 (UT) on 3 October 2005. (*b*) Concurrent AP data in the blue (left) and red (right) channels. Note that all the blue channel signals (left) reach saturation levels due to strong contamination from parent lightning.
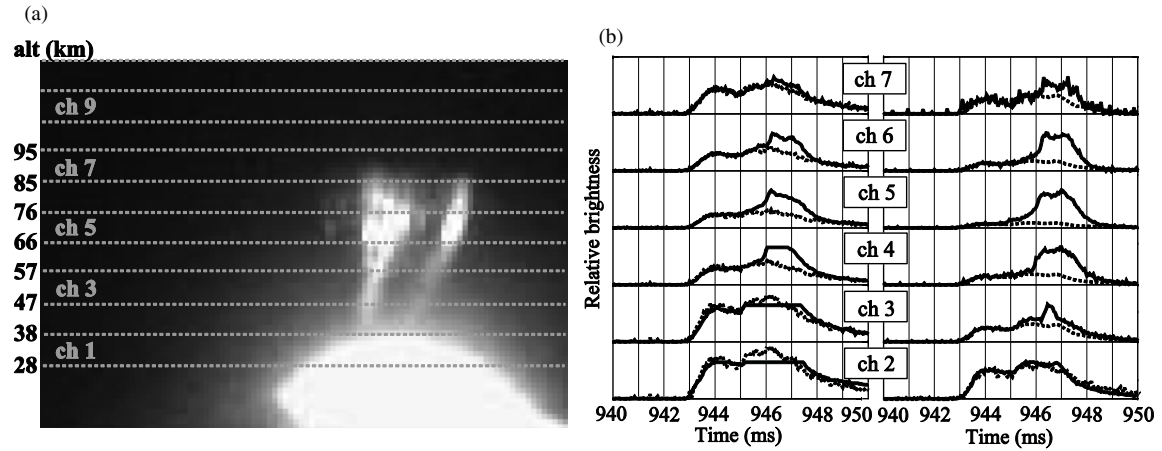
Figure 3. (*a*) An image of streamer event observed at 14:55:20.920-949 (UT) on 12 July 2005. (*b*) Concurrent AP data in the blue (left) and red (right) channels.

3. Electron energy and reduced electric field in sprites

The electron energy and electric field averaged in the FOV of each photometer channel and in time of 50 ms are derived from the blue to red (B/R) emission ratios observed by the AP (Adachi *et al* 2006). In this study, four band emission systems of nitrogen molecules and ions are assumed to be measured by the AP: N_2 second positive ($N_2$2P) band and N_2^+ first negative (N_2^+1N) band as the source of blue emissions, and N_2 first positive ($N_2$1P) band and N_2^+ Meinel (N_2^+MN) band as red emissions. Then, the B/R ratio is expressed as follows:

$$\frac{B}{R}\text{ratio} = \frac{I(N_2 2P) + I(N_2^+ 1N)}{I(N_2 1P) + I(N_2^+ 1MN)}. \tag{1}$$

Based on the assumption of uniform and quasi-steady electric field, the measured emission intensity I of each band system summed up with vibrational transitions ($v' \rightarrow v''$) is written as

$$I = N n_e \sum_{v'} \frac{k \cdot q_{v'} + g_{v'}}{\tau_{v'}^{-1} + k_q[M]} \sum_{v''} A_{v'v''} T(\lambda_{v'v''}) S(\lambda_{v'v''}), \tag{2}$$

where N and n_e are neutral and electron densities, k is the excitation rate coefficient, A is the Einstein spontaneous transition probability and τ, q, g is the lifetime, the Franck–Condon factor and the cascade effect of the upper vibrational level v', respectively. The quantity k_q is the collisional quenching coefficient and $[M]$ is the density of the quencher M ($= N_2$ or O_2). And T and S are the atmospheric transmittance and the absolute sensitivity of the AP, respectively, as functions of the wavelength λ. Here, T is calculated with the MODTRAN-4 code. The calculated transmittance for the ISUAL measurements is ~99.8% on average while that for the ground-based measurements is ~65%. Thus, it is evident that spectral measurements from space are preferable to precisely derive B/R ratios and to accurately estimate electric field intensities which produce the optical emissions of sprites. The value of k_q is given by Vallance Jones (1974), while τ, q, A and λ are taken from Gilmore *et al* (1992). The electronic transition from $C^3\Pi_u$ to $B^3\Pi_g$ is considered as a cascade term g of I($N_2$1P), or $g = 0$. For simplicity, all nitrogen molecules are assumed to be in the ground electronic and vibrational state before the impact of electrons. The value of k (see in figure 4),
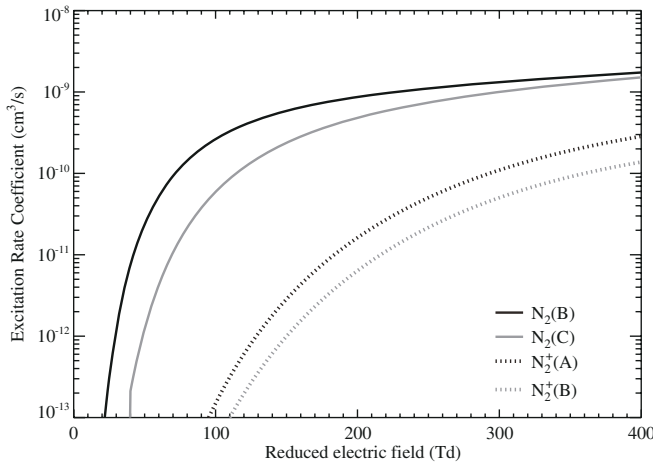
Figure 4. Excitation rate coefficients of first positive (black solid line) and second positive (grey solid line) bands of nitrogen molecules and Meinel (black dotted line) and first negative (grey dotted line) bands of nitrogen ions.

Figure 5. Sprite spectrum computed for reduced electric field of 300 Td and altitude of 80 km (black vertical lines) and the absolute sensitivity of AP at channel 8 (grey lines).

which is a function of the reduced electric field E/N, is solved with Monte Carlo swarm experiment (Hiraki and Fukunishi 2006) by following the equation

$$k = \int \sigma \sqrt{2\frac{E}{m_e}} f\left(\frac{E}{N}\right) dE, \qquad (3)$$

where σ is the total excitation cross section from the ground state, m_e is the mass of an electron and f is the electron energy distribution function. Because the time scale for electrons to reach the equilibrium state ($10\,\mu s$ or less at $90\,km$) is significantly shorter than that of an electric field induced by lightning (1–10 ms as shown in figure 9), the assumption of steady-state electric field is valid. On the basis of local field approximation, the kinetic equations of electrons including both elastic and inelastic collision processes are solved under electric fields in the wide range. However, it should be noted here that the electron energy distribution in a streamer head at a given field could deviate substantially from that of a space-charge-free electron swarm in the same electric field (e.g. Li *et al* 2007). Although such an effect might not be so critical in this study since the observed emissions come from both the heads of propagating streamers and the stationary structures in their trails as discussed later, it should be paid more attention in future experimental studies that treat spectrum of pure streamer heads. Because the production and loss terms of the excited state in equation (2) depend on k and $[M]$, respectively, the B/R ratio is a function of E/N and altitude. Figure 5 represents an example of a sprite spectrum computed for a reduced electric field of 300 Td and an altitude of 80 km while figure 6 shows the resultant B/R ratios calculated at channel 8. In order to estimate the altitude range covered by each photometer channel, it is assumed that the upper limit of the sprite altitude is 85 km and the altitude of the maximum intensity of lightning flash is 15 km, which is a typical altitude of thundercloud top at low latitudes where most sprites are observed by ISUAL.
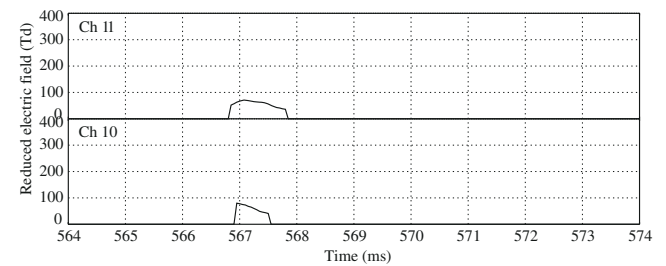
In this study, 25 streamer events and four halo events are used for the analysis. Here, the criteria of event selection
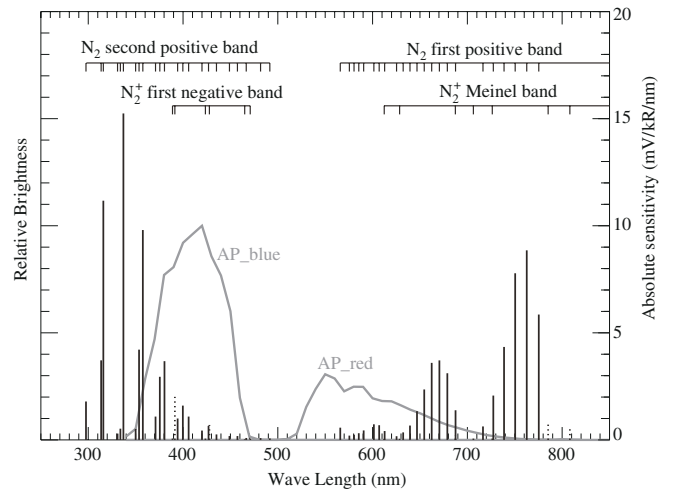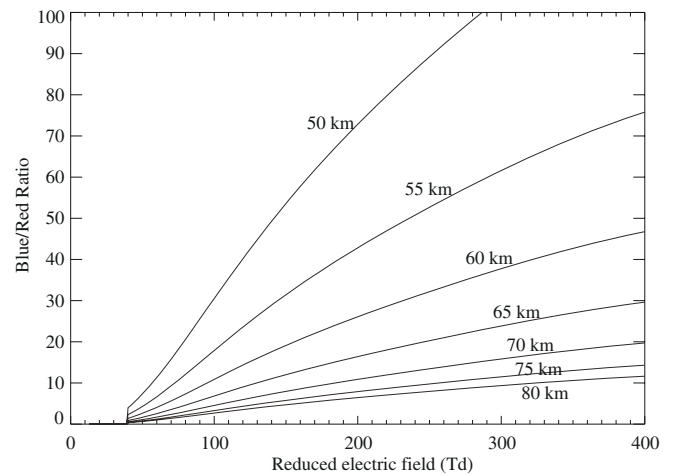
Figure 6. Modelled blue to red emission ratios as functions of reduced electric field and altitude for channel 8.

Figure 7. Reduced electric field estimated for a halo event observed at 04:40:25 (UT) on 9 October 2005.

are signal-to-noise ratios of $>10\sigma$ in both the AP red and blue filter channels, where σ is the standard deviation of background noise. Figure 7 represents an example of temporal evolution of reduced electric fields in a halo event. This halo is observed at 04:40:25 (UT) on 12 July 2005 and is the same event as that of figure 1. The estimated values reach maximum intensity initially and slightly decay during 1 ms. The initial peak

J. Phys. D: Appl. Phys. **41** (2008) 234010

T Adachi *et al*
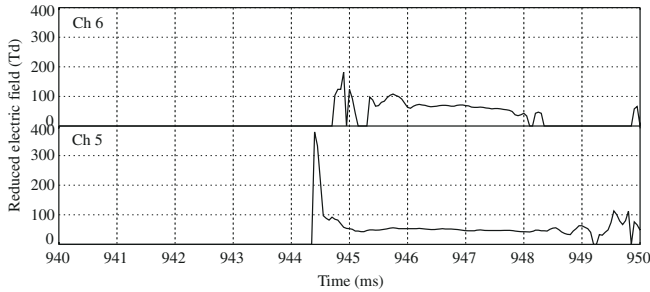
Figure 8. Reduced electric field estimated for a streamer event observed at 14:55:20 (UT) on 12 July 2005. The electric field in the lower channel shows up earlier than the upper channel, indicating the upward propagating streamers (cf Cummer *et al* 2006a).

values are 80–90 Td, which is significantly lower than the conventional dielectric breakdown field of ~128 Td (Hiraki and Fukunishi 2006). On the other hand, figure 8 is an example of the reduced electric fields in a streamer event, which is the same event as that of figure 3. In contrast to the halo event in figure 7, it is apparent that the reduced electric fields have initial transient enhancements of 200–400 Td, which suggest that strong ionization happens at the initiation of sprite streamers. The following fields are comparable to that of halo events but last for a longer time, as much as 3–6 ms. It should be noted here that the estimated values correspond to the electric fields that are substantially involved in producing optical emissions of sprite streamers and halos. Since halo events are not accompanied by a dielectric breakdown process, the estimated electric fields roughly reflect the background field induced by lightning discharges. However, since the streamer events are accompanied by the breakdown process that eventually causes the growth of streamers, the estimated electric fields are those inside the propagating streamers including the significant intensification at the channel tip.

Table 1 represents a summary of the initial peak reduced electric fields and concurrent average electron energies. Since the quenching term depends on the quencher density $[M]$, the modelled B/R ratio is sensitive to the assumed altitude. The quenching rate increases exponentially as the altitude decreases and, therefore, the errors in the assumed altitude make larger uncertainties in the electric fields at lower altitudes. Given an uncertainty of 10 km in the topside altitude of sprites (Sentman *et al* 1966), the errors of electric fields are ±5 Td at 80 km and ±50 Td at 60 km.

In the halo events, the initial peak electric fields are in the range 70–97 Td with an average of 81 Td while electron energies are 3.2–4.3 eV with an average of 3.8 eV. Here, the conventional breakdown field E_k of ~128 Td is defined as the electric field at which the ionization and attachment rate coefficients are balanced, and the attachment process dominates at $E < E_k$ while ionization dominates at $E > E_k$. Because the estimated fields are lower than E_k, significant ionization would not happen in the halo events. It is worth examining here if the optical emissions of halos could be observable at 70–97 Td where the breakdown does not occur. As shown in figure 4, the excitation rate coefficients of the $N_2\ B\ ^3\Pi_g$ state (the upper electronic state of the $N_2$1P band) are $1.6 \times 10^{-10}\ cm^3\ s^{-1}$ at 80 Td (0.6 E_k) and $4.0 \times 10^{-10}\ cm^3\ s^{-1}$

at 128 Td (1.0 E_k). On the other hand, those of the $N_2\ C\ ^3\Pi_u$ state (those of $N_2$2P band) are $2.0 \times 10^{-11}\ cm^3\ s^{-1}$ at 80 Td and $1.5 \times 10^{-10}\ cm^3\ s^{-1}$ at 128 Td. Thus, the ratio of the rate coefficients at 0.6 E_k to those at E_k is no less than ~0.4 for the $N_2\ B\ ^3\Pi_g$ state and ~0.1 for the $N_2\ C\ ^3\Pi_u$ state. Since optical instruments typically used for sprite measurements have order-of-magnitude dynamic ranges, it is concluded that optical emissions of nitrogen molecules ($N_2$1P and $N_2$2P) are observable even at $E \sim 0.6E_k$. Consequently, the results obtained suggest that the electric field required for the production of a halo is in the range 70–100 Td, which is consistent with the theoretical expectation by Hiraki and Fukunishi (2006).

On the other hand, the initial peak values of reduced electric fields (and average electron energy) of streamer events are 59–149 Td (2.8–5.3 eV) with an average of 84 Td (3.9 eV) in the upper-diffuse region and are 98–380 Td (4.4–8.9 eV) with an average of 176 Td (5.8 eV) in the lower-structured region. Therefore, since the estimated fields are higher than the breakdown field (~128 Td), significant ionization happens at the initiation of the structured region of streamer events. However, a recent experimental study based on ISUAL SP data has estimated peak electric fields of 243–443 Td, which is consistent with the theoretical prediction of streamer head (Liu *et al* 2004) but is two times higher than our estimation. This discrepancy would come from the difference of the observed wavelength range. While the present analysis is primarily based on the broadband emissions of the $N_2$1P (red) and $N_2$2P (blue) bands, their analysis was based on the narrowband emissions of the N_2^+1N and $N_2$2P bands. In figure 4 of Kuo *et al* (2005), it is apparent that the optical emission peaks happen in the order of N_2^+1N (SP3), $N_2$2P (SP2) and $N_2$1P (SP4). Therefore, the electric fields derived from the blue ($N_2$2P) to the red ($N_2$1P) emission ratios in this study correspond to the later stage while those derived from the $N_2$2P to N_2^+1N ratios in Kuo *et al* (2005) correspond to the earlier stage.

It has been reported that the streamer modelling agrees well with the ISUAL SP measurements at the initial sprite development stage (up to ~0.5 ms) but might not be applicable at the later stage (Liu *et al* 2006). In this study, the estimated electric fields, which probably correspond to the later stage, are also two or three times lower than those in the streamer head predicted in models. High-speed imaging observations (Cummer *et al* 2006a, McHarg *et al* 2007) have revealed that sprite streamers initially propagate downwards branching into multiple channels and decay with a lifetime of ~0.8 ms, which is comparable to the time scale of the initial stage where the streamer modelling agrees well with the experimental results. Subsequently, streamers propagate upwards from the branching altitude and finally form the later bright stage with stationary structures which continue glowing in the trails of the streamers. The fact that the initial peak electric fields estimated in this study are lower than those in the modelled streamer head is probably because the measured optical emissions come from both the fast-moving streamer heads and the stationary structures in their trails. For the full consistency between the theory and observation especially at the later bright and stationary stage of sprites, chemical processes might be one of

Table 1. A summary of peak magnitudes of reduced electric fields and average electron energies.

Category	Reduced electric field (Td)		Average electron energy (eV)	
	Range	Average	Range	Average
Halo	70–97	81	3.2–4.3	3.8
Halo-streamer	N/A[a]	N/A[a]	N/A[a]	N/A[a]
Streamer				
>75 km diffuse region	59–149	84	2.8–5.3	3.9
<75 km structured region	98–380	176	4.4–8.9	5.8

[a] The values are not available because the strong contamination from parent lightning flash causes significant saturation especially in the blue photometer channels (see figure 2(*b*), left panels).

the most essential keys as has been discussed by Sentman *et al* (2008).

4. Temporal evolution of lightning charge moment

Temporal evolutions of lightning charge moment changes are estimated using the AP photometric data and ELF magnetic field data. As seen in figures 1–3, the AP is able to separately detect optical emissions of TLEs and lightning. Temporal evolution of lightning luminosity $L(t)$ observed by the red channels of AP is integrated with time and normalized using the following equation:

$$R(t) = \frac{\int_0^t L(t)\,\mathrm{d}t}{\int_0^\infty L(t)\,\mathrm{d}t}. \tag{4}$$

Past optical and electromagnetic measurements have found that brightness of lightning return stroke is linearly correlated with the magnitude of the electric current (Jordan and Uman 1983, Idone and Orville 1985). Their results suggest that lightning luminosity, $L(t)$, probably represents the temporal evolution of electric current intensity. Consequently, given that the altitude of thundercloud charge is invariable during the discharge time of a few milliseconds, the $R(t)$ would correspond to the relative temporal variation of charge moment change.

It would be worth noting here that the relationship between the lightning luminosity and the corresponding current intensity might be more complicated than the assumed proportionality at least in the time scale of tens of microseconds (e.g. Wang *et al* 2005). At the same time, a clear correlation between the luminosity and the electromagnetic wave, from which one can extract the current moment, has been found in the millisecond scale (see figure 4, Cummer *et al* 2006b). Therefore, although the method of analysis used in this study could be applicable for millisecond-scale discussions, further experiments are required to clarify the luminosity–current relationship.

The absolute values of time-integrated charge moments are calculated from transient SR data with an analytical technique described by Huang *et al* (1999). The frequency-dependent complex magnetic field, $H_\Phi(f)$, measured with orthogonal magnetometers at the Onagawa observatory is a function of the source current moment spectrum, $I(f)l$, as expressed in the following equation:

$$H_\Phi(f) = -\frac{I(f)l\,P_m^1(-\cos\theta)}{4ah\sin(\pi\nu)}. \tag{5}$$

Here, $P_\nu^1(\cos\theta)$ is the Legendre polynomials with a harmonics order m and first degree, θ is the angular distance between the CG discharge and the receiver, $a = 6378$ km is the radius of the Earth, $h = 80$ km is the height of the ionospheric reflection boundary, and ν is the complex eigenvalue derived from the equation shown in Ishaq and Jones (1977) that describes the characteristics of propagation and dissipation. For the estimation of charge moment, the temporal variation of lightning current moment is assumed to be of an exponential form in the time domain as shown in equation (6). The complex current moment spectrum expressed in equation (7) is obtained from the Fourier transform of the current moment waveform:

$$I(t)l = I_\mathrm{o}l\exp\left(\frac{-t}{\tau}\right), \tag{6}$$

$$I(f)l = \frac{I_\mathrm{o}l}{2\pi f + \tau^{-1}}. \tag{7}$$

The parameter τ, corresponds to the decay time constant of lightning current. As shown in figures 1–3, the typical lifetime of a lightning flash is a few milliseconds, which suggests that the decay time constant of sprite-producing lightning is shorter than the period of the SR wave in the first mode ($\sim$125 ms). Therefore, by assuming $2\pi f \ll \tau^{-1}$, equation (7) is rewritten as follows:

$$I(f)l = I_\mathrm{o}l\tau = Ql. \tag{8}$$

Consequently, the time-integrated charge moment value Ql can be directly derived from the current moment spectrum $I(f)l$ based on the assumption of impulsive lightning currents.

It should be noted that this method of analysis has an ambiguity in the estimation of charge moment changes. It has been reported that the charge moment values derived from SR data are roughly 30% lower than those derived from ELF/VLF sferics data (Sato and Fukunishi 2003). Furthermore, by performing the cross-checks between the charge moment changes derived from SR data obtained at the Onagawa observatory and those simultaneously obtained at the Syowa station (69.0°S, 39.6°E) in Antarctica, the accuracy of the analytical technique is investigated. It is found that the charge moment values estimated from these two different datasets had random differences of 200–300%. Consequently, a systematic error of −30% and a random error of 200–300% are expected in the estimated charge moment changes in this study.

By combining the temporal evolution of relative lightning luminosity, $R(t)$, derived from the ISUAL measurement with the time-integrated absolute charge moment Ql estimated from

J. Phys. D: Appl. Phys. **41** (2008) 234010

T Adachi *et al*
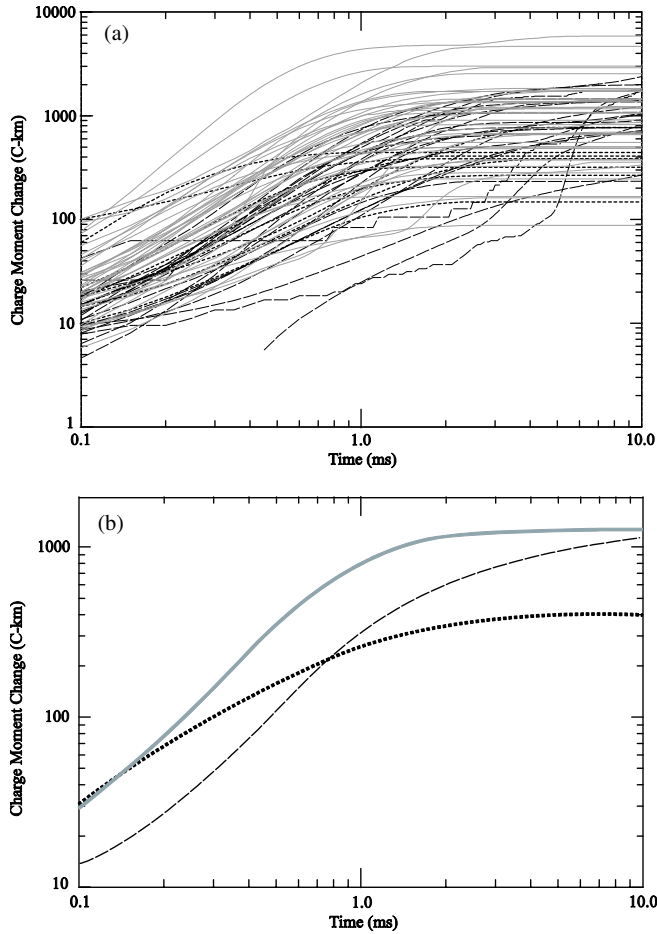
Figure 9. (*a*) Temporal evolution of charge moment changes in 69 sprite events. Black dotted lines represent eight halo events, grey solid lines represent 39 halo-streamer events, and black dashed lines represent 22 streamer events. (*b*) Temporal evolution of charge moment charges averaged in each category.

Table 2. Average time scales and charge moment changes of lightning discharges in each category.

Category	Time scale	Total charge moment
Halo	$\sim$1 ms	$\sim$400 C km[a]
Halo-streamer	$\sim$1 ms	$\sim$1300 C km[a]
Streamer	$\sim$10 ms	$\sim$1300 C km[a]

[a] The systematic error of -30% in the SR analysis is corrected.

the order-of-magnitude variations in each category found in figure 9(*a*).

In order to clearly indicate the characteristics of each category, averaged $Ql(t)$ are shown in figure 9(*b*). Temporal evolutions of charge moment changes are evidently different between each category. In the halo event (black dotted line), the values of $Ql(t)$ are relatively high during the initial 1 ms but relatively low during the following period, which suggest a rapid removal of a moderate amount of thundercloud charge. In the halo-streamer event (grey solid line), the values of $Ql(t)$ are highest during the entire period, implying a rapid removal of a large amount of thundercloud charge. In contrast to the other two categories, temporal evolution of $Ql(t)$ in the streamer events (black dashed line) has a long time scale. The values of $Ql(t)$ continue increasing for 10 ms and finally reach almost the same value as the halo-streamer events, which suggests a slow removal of a large amount of thundercloud charge. Table 2 represents the total charge moment changes and the timescales required to reach half values. In the case that the time scale is short ($\sim$1 ms), it is found that lightning discharges with a charge moment value of $\sim$400 C km produce sprite halos while lightning discharges with $\sim$1300 C km produce sprite streamers besides halos. On the other hand, lightning discharges with a long time scale ($\sim$10 ms) and a large charge moment change ($\sim$1300 C km) are found to produce streamers without discernible halos.

5. Discussion

Based on the obtained results, the fundamental electrodynamical coupling processes between sprites and lightning are discussed. As represented in section 3, the initial peak electric fields in sprite halos are $\sim$80 Td or $\sim$0.7 E_k, which suggest that the necessary condition of halos is not the dielectric breakdown process but is the production of optical emissions via the electron impact excitation of the neutral atmosphere. Since A and N are invariable with time, the brightness of sprite halo, which is expressed as $Ak(E/N)Nn_e$, is a function of $k(E/N)$ and $n_e(t)$. When the electric field is applied, accelerated electrons collide with the neutral particles (mainly with N_2 and O_2), causing the processes of excitation, ionization and attachment. The essential processes for the number of electrons are impact ionization and dissociative attachment. Thus, the net production/reduction of electron density is controlled by the balance of these two processes and is expressed by the following equation:

$$\frac{dn_e}{dt} = (k_{ion} - k_{att})Nn_e. \tag{10}$$

the ELF magnetic field measurement, the temporal evolution of charge moment changes $Ql(t)$ are estimated as follows:

$$Ql(t) = Ql \cdot R(t). \tag{9}$$

Here, the starting time $t = 0$ is set when the lightning luminosity for the first time exceeds the level five times higher than the standard deviation σ of background noise level.

In this study, 69 sprite events are analysed in which both the photometric (AP red channels) and magnetic field data have sufficient signal-to-noise ratios ($>10\sigma$). The obtained results are shown in figure 9(*a*), in which the systematic error of -30% is corrected. Out of 69 sprite events, eight events are halos (black dotted lines), 39 events are halo with streamers (grey solid lines) and 22 events are streamers (black dashed lines). It is apparent that the event-to-event variations of $Ql(t)$ are significantly large in each category. The ratios of the maximum values to the minimum values are $\sim$5 in halo events $\sim$60 in halo-streamer events, and $\sim$10 in streamer events. Although these variations are primarily due to the errors in the analysis, some factors such as seasonal and regional variations might play additional roles because the expected random error of 200–300% is insufficient to fully explain

Here, k_{ion} and k_{att} are the ionization and dissociative attachment rate coefficients, respectively. As discussed in section 3, the attachment process dominates at $E < E_k$ while ionization dominates at $E > E_k$. Since the peak reduced electric fields are lower than E_k, k_{att} is larger than k_{ion} both before and during the occurrence of halos. Thus, it is apparent that equation (10) is rewritten as $dn_e/dt < 0$, suggesting a significant reduction of electrons. By considering that the brightness of halos is proportional to $k(E/N)$ and $n_e(t)$, it is clear that larger $k(E/N)$ is required with time for the production of a sprite halo because the electron density $n_e(t)$ decreases with time. Since $dk_B/d(E/N)$ is positive as shown in figure 5, the critical electric field for the production of a discernible halo, E_1, also increases with time. On the other hand, the initial peak electric fields in the structured region of sprites are found to be higher than E_k. It is, therefore, suggested that the dielectric air breakdown occurs and the ionization dominates the attachment. Numerical calculations solving the kinetics in streamers have represented that strong ionization drives the electron avalanche process, resulting in the formation of filamentary plasma structures within a certain amount of time (a few milliseconds at the mesospheric altitudes) (e.g. Pasko *et al* 1998, Liu and Pasko 2004). The results obtained in this study also indicate that significant ionization happens at the initiation of sprite streamers. Consequently, the critical field necessary for the formation of a sprite streamer is the conventional air breakdown field E_k. In contrast to E_1, it is worth noting here that the dielectric breakdown field, E_k, is invariable with time.

In summary, the critical field for the production of streamers is the conventional breakdown field of 128 Td which is invariable with time. On the other hand, the critical field of a halo would be ~80 Td initially but increases significantly with time due to the reduction of electrons. Simple calculations with equation (10) and the values of k_{ion} and k_{att} taken from Hiraki and Fukunishi (2006) suggest that E_1 is lower than E_k in the case of a quickly-applied thundercloud electric field ($t \ll 1$ ms), while E_1 is higher than E_k in the case of a slowly applied field ($t \gg 1$ ms).

The applied electric fields calculated from lightning charge moment changes are compared with the critical fields of both phenomena. In the halo events, it is found in section 4 that lightning discharges have a time scale of ~1 ms and a total charge moment value of ~400 C km, which can quickly induce moderately intense electric fields above thunderstorms. Because significant attachment (time scale is 2–3 ms at 85 km (e.g. Pasko *et al* (1998)) would not occur, it is expected that the critical fields of halos E_l and streamers E_k stay at ~80 Td and ~128 Td, respectively. Using a simple dipole model with a cloud charge Q left at an altitude of l above a perfectly conducting ground, the applied electric field at an altitude z along the axis of source charge is expressed as follows (cf Raizer *et al* (1998)):

$$E(z) = \frac{Ql}{\pi \varepsilon_0 z^3}. \tag{11}$$

Here, $\varepsilon_0 = 8.85 \times 10^{-12}$ A^2 s^2 N^{-1} m^{-2} is the permittivity in vacuum. In the case that charge moment value Ql is 400 C km, the

electric field intensity calculated from equation (11) is ~83 Td at an altitude of 80 km. Consequently, since $E_1 \sim 80$ Td $< E < E_k \sim 128$ Td, it is reasonable that lightning discharges in this category produce sprite halos only.

In the halo-streamer events, lightning discharges are found to have a time scale of ~1 ms and total charge moment changes of ~1300 C km. In a similar manner, the critical electric fields of halos and streamers are expected to stay ~80 Td and ~128 Td, respectively, because the lightning time scale is relatively short so that the attachment process would be negligible. However, the estimated charge moment change of ~1300 C km in this category is much larger than that in the halo event, suggesting that a more intense electric field is applied. Actually, it is estimated from equation (11) that an electric field of ~267 Td is applied at an altitude of 80 km. Thus, because $E_1 < E_k < E$, it is reasonable that the lightning discharges in this category produce sprite streamers besides sprite halos.

In contrast to the other two categories, lightning discharges in the streamer events have a time scale of ~10 ms. Since slowly applied electric fields would decrease electron density through the attachment process, the critical field of halos would increase rapidly with time. If the net attachment rate, $k_{att} - k_{ion}$, can be assumed as 3×10^{-12} cm^3 s^{-1} for simplicity (figure 1(*a*) of Hiraki and Fukunishi (2006)), it is expected from equation (10) that the increasing time scale of E_1 at 80 km is ~1 ms. Therefore, the value of E_1 is expected to reach the level of $\gg 600$ Td at ~10 ms while the breakdown field E_k stays at ~128 Td. On the other hand, from equation (11), lightning-induced electric fields at 80 km are calculated as ~267 Td in the case of $Ql \sim 1300$ C km. Consequently, since $E_k < E < E_1$, it is reasonable that lightning discharges in this category produce sprite streamers without discernible halos.

6. Conclusions

Based on the satellite-based spectral measurements and simultaneous ground-based electromagnetic measurements, electrodynamical coupling processes between lightning discharges and sprites are comprehensively studied. The principal results obtained in this study are summarized as follows.

1. On the basis of broadband blue to red emission ratios observed with the ISUAL AP, spatiotemporal-resolved reduced electric fields are estimated. The maximum intensities of electric fields (and average electron energies) in halo events are found to be 70–97 Td (3.2–4.3 eV), which are lower than the conventional breakdown field $E_k \sim 128$ Td. On the other hand, those of streamer events are found to be 59–149 Td (2.8–5.3 eV) in the upper-diffuse region and 98–380 Td (4.4–8.9 eV) in the lower-structured region, which indicates that significant ionization happens in the formation of streamers.
2. By combining the AP data with the ELF magnetic field data, temporal evolutions of lightning charge moment changes are estimated. It is found that the lightning discharge producing a halo without streamers has a short time scale of ~1 ms with a moderate charge moment of ~400 C km while that producing streamers as well as a

halo have a similar time scale of ∼1 ms but a large charge moment of ∼1300 C km. On the other hand, a lightning discharge producing sprite streamers without a discernible halo has a long time scale of ∼10 ms and a large charge moment of ∼1300 C km.

3. The obtained results are interpreted considering the necessary conditions for sprite streamers and halos. The necessary field of streamers is the conventional breakdown field, $E_k \sim 128$ Td, while that of halos, E_l, would be ∼80 Td under the initial ambient electron density. However, since the electron density would decrease if the thundercloud electric field is applied slowly, significantly higher E_l is required for the production of a halo. Thus, only the lightning discharge with a short time scale can produce a sprite halo. On the other hand, since the necessary field of streamers, E_k, is invariable with time, all the lightning discharges with a large charge moment can produce streamers regardless of the time scale.

Acknowledgments

References

Adachi T, Fukunishi H, Takahashi Y, Chen A B, Mende S B, Frey H U and Lee L C 2006 Electric field transition between the diffuse and streamer regions of sprites estimated from ISUAL/array photometer measurements *Geophys. Res. Lett.* **33** L17803

Barrington-Leigh C P, Inan U S and Stanley M 2001 Identification of sprites and elves with intensified video and broadband array photometer *J. Geophys. Res.* **106** 1741–50

Chern J L, Hsu R R, Su H T, Mende S B, Fukunishi H, Takahashi Y, and Lee L C 2003 Global survey of upper atmospheric transient luminous events on the ROCSAT-2 satellite *J. Atmos. Sol. Terr. Phys.* **65** 647–59

Cummer S A and Inan U S 1997 Measurement of charge transfer in spriet-producing lightning using ELF radio atmospherics *Geophys. Res. Lett.* **24** 1731–4

Cummer S A, Jaugey N, Li J, Lyons W A, Nelson T E and Gerken E A 2006a Submillisecond imaging of sprite development and structure *Geophys. Res. Lett.* **33** L04104

Cummer S A, Frey H, Mende S B, Hsu R-R, Su H-T, Chen A B, Fukunishi H and Takahashi Y 2006b Simultaneous radio and satellite optical measurements of high-altitude sprite current and lightning continuing current *J. Geophys. Res.* **111** A10315

Füllekrug M and Reising S C 1998 Excitation of Earth-ionosphere cavity resonances by sprite-associated lightning flashes *Geophys. Res. Lett.* **25** 4145–8

Frey H U, Mende S B, Cummer S A, Chen A B, Hsu R-R, Su H-T, Chang Y-S, Adachi T, Fukunishi H and Takahashi Y 2005 Beta-type stepped leader of elve-producing lightning *Geophys. Res. Lett.* **32** L13824

Frey H U, Mende S B, Cummer S A, Li J, Adachi T, Fukunishi H, Takahashi Y, Chen A B, Hsu R-R, Su H-T and Chang Y-S 2007 Halos generated by negative cloud-to-ground lightning *Geophys. Res. Lett.* **34** L18801

Gerken E A, Inan U S and Barrington-Leigh C P 2000 Telescopic imaging of sprites *Geophys. Res. Lett.* **27** 2637–40

Gerken E A and Inan U S 2002 A survey of streamer and diffuse glow dynamics observed in sprits using telescopic imagery *J. Geophys. Res.* **107** 1344

Gilmore F R, Laher R R and Espy P J 1992 Franck-Condon factors, *r*-centroids, electronic-transition moments, and Einstein coefficients for many nitrogen and oxygen band systems *J. Phy. Chem. Ref. Data* **21** 1005–107

Green B D, Fraser M E, Rawlins W T, Jeong L, Blumberg W A M, Mende S B, Swenson G R, Hampton D L, Wescott E M and Sentman D D 1996 Molecular excitation in sprites *Geophys. Res. Lett.* **23** 2161–4

Hampton D L, Heavner M J, Wescott E M and Sentman D D 1996 Optical spectral characteristics of sprites *Geophys. Res. Lett.* **23** 89–92

Hiraki Y and Fukunishi H 2006 Theoretical criterion of charge moment change by lightning for initiation of sprites *J. Geophys. Res.* **111** A11305

Hu W, Cummer S A, Lyons W A and Nelson T E 2002 Lightning charge moment changes for the initiation of sprites *Geophys. Res. Lett.* **29** 1279

Huang E, Williams E, Boldi R, Heckman S, Lyons W, Taylor M, Nelson T and Wang C 1999 Criteria for sprites and elves based on Schumann resonance observations *J. Geophys. Res.* **104** 16943–64

Hobara Y, Iwasaki N, Hayashida T, Hayakawa M, Ohta K and Fukunishi H 2001 Interrelation between ELF transients and ionospheric disturbances in association with sprites and elves *Geophys. Res. Lett.* **28** 935–8

Idone V P and Orville R E 1985 Correlated peak relative light intensity and peak current in triggered lightning subsequent return strokes *J. Geophys. Res.* **90** 6159–64

Ishaq M and Jones D L 1977 Method of obtaining radiowave propagation parameters for the Earth-ionosphere duct at E.I.F. *Electron. Lett.* **13** 254–5

Jordan D M and Uman M A 1983 Variation in light intensity with height and time from subsequent lightning return strokes *J. Geophys. Res.* **88** 6555–62

Kuo C L, Hsu R R, Chen A B, Su H T, Lee L C, Mende S B, Frey H U, Fukunishi H and Takahashi Y 2005 Electric fields and electron energies inferred from the ISUAL recorded sprites *Geophys. Res. Lett.* **32** L19103,

Li C, Brok W J M, Ebert U and van der Mullen J J A M 2007 Deviations from the local field approximation in negative streamer heads *J. Appl. Phys.* **101** 123305

Liu N and Pasko V P 2004 Effects of photoionization on propagation and branching of positive and negative streamers in sprites *J. Geophys. Res.* **109** A04301

Liu N, Pasko V P, Burkhardt D H, Frey H U, Mende S B, Su H T, Chen A B, Hsu R R, Lee L C, Fukunishi H and Takahashi Y 2006 Comparison of results from sprite streamer modeling with spectrophotometric measurements by ISUAL instrument on FORMOSAT-2 satellite *Geophys. Res. Lett.* **33** L01101

McHarg M G, Stenbaek-Nielsen H C and Kammae T 2007 Observations of streamer formation in sprites *Geophys. Res. Lett.* **34** L06804

Mende S B, Rairden R L, Swenson G R and Lyons W A 1995 Sprite spectra: N₂ first positive band identification *Geophys. Res. Lett.* **22** 2633–6

Mende S B, Frey H U, Hsu R-R, Su H-T, Chen A B, Lee L C, Sentman D D, Takahashi Y and Fukunishi H 2005 D region ionization by lightning-induced electromagnetic pulses *J. Geophys. Res.* **110** A11312

Miyasato R, Taylor M J, Fukunishi H and Stenbaek-Nielsen H C 2002 Statistical characteristics of sprite halo events using coincident photometric and imaging data *Geophys. Res. Lett.* **29** 2033

Miyasato R, Fukunishi H, Takahashi Y and Taylor M J 2003 Energy estimation of electrons producing sprite halos using array photometer data *J. Atmos. Sol. Terr. Phys.* **65** 573–81

Morrill J S, Bucsela E J, Pasko V P, Berg S L, Heavner M J, Moudry D R, Benesch W M, Wescott E M and Sentman D D 1998 Time resolved N_2 triplet state vibrational populations and emissions associated with red sprites *J. Atmos. Sol. Terr. Phys.* **60** 811–29

Moudry D R, Stenbaek-Nielsen H C, Sentman D D and Wescott E M 2003 Imaging of elves, halos and sprite initiation at 1 ms time resolution *J. Atmos. Sol. Terr. Phys.* **65** 509–18

Pasko V P, Inan U S and Bell T F 1998 Spatial structure of sprites *Geophys. Res. Lett.* **25** 2123–6

Pasko V P and Stenbaek-Nielsen H C 2002 Diffuse and streamer regions of sprites *Geophys. Res. Lett.* **29** 1440

Raizer Y P, Milikh G M, Shneider M N and Novakovski S V 1998 Long streamers in the upper atmosphere above thundercloud *J. Phys. D: Appl. Phys.* **31** 3255–64

Sato M and Fukunishi H 2003 Global sprite occurrence locations and rates derived from triangulation of transient Schumann resonance events *Geophys. Res. Lett.* **30** 1859

Sentman D D, Wescott E M, Osborne D L, Hampton D L and Heavner M J 1995 Preliminary results from the Sprites94 aircraft campaign: I. Red sprites *Geophys. Res. Lett.* **22** 1205–8

Sentman D D 1996 Schumann resonance spectra in a two-scale-height Earth-ionosphere cavity *J. Geophys. Res.* **101** 9479–87

Sentman D D, Stenbaek-Nielsen H C, McHarg M G and Morrill J S 2008 Plasma chemistry of sprite streamers *J. Geophys. Res.* **113** D11112

Suszcynsky D M, Roussel-Dupré R, Lyons W A and Armstrong R A 1998 Blue-light imagery and photometry of sprites *J. Atmos. Sol. Terr. Phys.* **60** 801–10

Vallance Jones A V 1974 *Aurora* (New York: Springer)

Wang D, Takagi N, Watanabe T, Rakov V A, Uman M A, Rambo K J and Stapleton M V 2005 A comparison of channel-base currents and optical signals for rocket-triggered lightning strokes *Atmos. Res.* **76** 412–22

Wescott E M, Sentman D D, Heavner M J, Hampton D L, Lyons W A, Nelson T 1998 Observations of 'Columniform' sprites *J. Atmos. Sol. Terr. Phys.* **60** 733–40

Wescott E M, Stenbaek-Nielsen H C, Sentman D D, Heavner M J, Moudry D R and São Sabbas F T 2001 Triangulation of sprites, associated halos and their possible relation to causative lightning and micrometeors *J. Geophys. Res.* **106** 10467–77